GL-TR-89-0184

AD-A222 652

PRELIMINARY DEVELOPMENT OF OBLIQUE IONOGRAM

AUTOMATIC SCALING ALGORITHM

Walter S. Kuklinski
Kavitha Chandra
Bodo W. Reinisch

University of Lowell
Center for Atmospheric Research
450 Aiken Street
Lowell, Massachusetts   01854

October 1988

Scientific Report No. 13

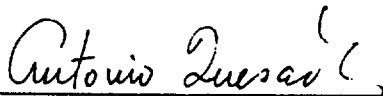Approved for public release; distribution unlimited.

90 06 12 131

"This technical report has been reviewed and is approved for publication"

_____   _____
ANTONIO QUESADA   WILLIAM K. VICKERY
Contract Manager   Branch Chief

FOR THE COMMANDER

_____
ROBERT A. SKRIVANEK
Division Director

This report has been reviewed by the ESD Public Affairs Office (PA) and is releasable to the National Technical Information Service (NTIS).

Qualified requestors may obtain additional copies from Defense Technical Information Center.

If your address has changed, or if you wish to be removed from the mailing list, or if the addressee is no longer employed by your organization, please notify AFGL/DAA, Hanscom AFB, MA 01731. This will assist us in maintaining current mailing list.

Do not return copies of this report unless contractual obligations or notice on a specific document requires that it be returned.

REPORT DOCUMENTATION PAGE

Form Approved
OMB No. 0704-0188

1a. REPORT SECURITY CLASSIFICATION	1b. RESTRICTIVE MARKINGS
Unclassified	

2a. SECURITY CLASSIFICATION AUTHORITY	3. DISTRIBUTION/AVAILABILITY OF REPORT
	Approved for public release;
2b. DECLASSIFICATION/DOWNGRADING SCHEDULE	distribution unlimited.

4. PERFORMING ORGANIZATION REPORT NUMBER(S)	5. MONITORING ORGANIZATION REPORT NUMBER(S)
ULRF-453/CAR	GL-TR-89-0184

6a. NAME OF PERFORMING ORGANIZATION	6b. OFFICE SYMBOL (If applicable)	7a. NAME OF MONITORING ORGANIZATION
University of Lowell		NorthWest Research Associates, Inc.

6c. ADDRESS (City, State, and ZIP Code)	7b. ADDRESS (City, State, and ZIP Code)
Center for Atmospheric Research	300 120th Avenue, NE
450 Aiken Street	Bellevue, WA 98005
Lowell, MA 01854	

8a. NAME OF FUNDING/SPONSORING ORGANIZATION	8b. OFFICE SYMBOL (If applicable)	9. PROCUREMENT INSTRUMENT IDENTIFICATION NUMBER
Geophysics Laboratory	LIS	F19628-87-C-0003

8c. ADDRESS (City, State, and ZIP Code)	10. SOURCE OF FUNDING NUMBERS			
Hanscom AFB	PROGRAM ELEMENT NO.	PROJECT NO.	TASK NO.	WORK UNIT ACCESSION NO.
Massachusetts 01731-5000	62101F	4643	10	AC

11. TITLE (Include Security Classification)

Preliminary Development of Oblique Ionogram Automatic Scaling Algorithm

12. PERSONAL AUTHOR(S)

Walter S. Kuklinski; Kavitha Chandra; Bodo W. Reinisch

13a. TYPE OF REPORT	13b. TIME COVERED	14. DATE OF REPORT (Year, Month, Day)	15. PAGE COUNT
Scientific #13	FROM _____ TO _____	1988 October	30

16. SUPPLEMENTARY NOTATION

17. COSATI CODES			18. SUBJECT TERMS (Continue on reverse if necessary and identify by block number)
FIELD	GROUP	SUB-GROUP	Oblique Ionograms Wiener Filter
			Algorithm Noise/Interference
			Vertical Ionogram Trace Enhancement

19. ABSTRACT (Continue on reverse if necessary and identify by block number)

Using vertical ionograms to quantitatively determine radio frequency (RF) propagation conditions is a mature and well established technique. In principle, a large number of scaled vertical ionograms, and the electron density profiles that can be derived from them, along a specific path of interest would be required to completely assess the RF propagation conditions for that path. Typically, the midpoint ionosphere is a good approximation of the ionosphere along a specific path of interest and RF propagation conditions for that path can be determined from the scaled midpoint vertical ionogram. The difficulty of placing the required sounding hardware at the midpoint of a desired path can be resolved by developing a system capable of calculating the equivalent scaled vertical ionogram at the midpoint of a specific path: Digital Oblique Remote Ionospheric Sensing (DORIS) program. A major component of DORIS is the development of an automatic scaling algorithm that can produce equivalent scaled midpoint vertical ionograms from oblique ionograms produced by a pair of Digisondes. (KR)K

20. DISTRIBUTION/AVAILABILITY OF ABSTRACT	21. ABSTRACT SECURITY CLASSIFICATION
☐ UNCLASSIFIED/UNLIMITED ☐ SAME AS RPT. ☐ DTIC USERS	Unclassified

22a. NAME OF RESPONSIBLE INDIVIDUAL	22b. TELEPHONE (Include Area Code)	22c. OFFICE SYMBOL
Antonio Quesada		GL/LIS

DD Form 1473, JUN 86   Previous editions are obsolete.   SECURITY CLASSIFICATION OF THIS PAGE

TABLE OF CONTENTS

DTIC
COPY
INSPECTED
6

Accession For

NTIS GRA&I	☑
DTIC TAB	☐
Unannounced	☐
Justification	

By____

Distribution/

Availability Codes

Dist	Avail and/or Special
A-1	

LIST OF FIGURES

iv

LIST OF FIGURES (Continued)

1.0 INTRODUCTION

Using vertical ionograms to quantitatively determine radio frequency (RF) propagation conditions is a mature and well established technique. In principle, a large number of scaled vertical ionograms, and the electron density profiles that can be derived from them, along a specific path of interest would be required to completely assess the RF propagation conditions for that path. Typically, the midpoint ionosphere is a good approximation of the ionosphere along a specific path of interest and RF propagation conditions for that path can be determined from the scaled midpoint vertical ionogram. Previously this has required recording a vertical ionogram at the desired midpoint, scaling the vertical ionogram and if desired inverting the scaled vertical ionogram to obtain an electron density profile. The difficulty of placing the required sounding hardware at the midpoint of a desired path can be resolved by developing a system capable of calculating the equivalent scaled vertical ionogram at the midpoint of a specific path of interest from any oblique ionogram with the same midpoint. A major component of the Digital Oblique Remote Ionospheric Sensing (DORIS) program, is the development of an automatic scaling algorithm that can produce equivalent scaled midpoint vertical ionograms from oblique ionograms produced by a pair of Digisondes. The wide range of variations that can reasonably be expected to be present in oblique ionograms recorded during disturbed and normal ionospheric conditions will require an increased level of sophistication compared to that used for automatic scaling of vertical ionograms recorded at identical ionospheric conditions. The existence of a reliable, well tested vertical ionogram scaling algorithm Automatic Real-Time Ionogram Scaling and True-Height (ARTIST) calculation, as part of the Digisonde 256 will, however, allow adaptive techniques to be utilized in the development of the oblique ionogram scaling algorithm. While the specific details of the final functional oblique

ionogram scaling algorithm will depend on a number of system factors (e.g. oblique path geography, availability of polarization data, transmit power and waveforms), application of adaptive signal processing and pattern recognition techniques will provide adequate flexibility to incorporate the present off-line oblique ionogram scaling algorithm with existing Digisonde 256 software and hardware.

2.0 APPROACH

The oblique ionogram scaling algorithm can be represented as a number of separate but interrelated functional operations including: noise/interference suppression; trace enhancement; trace identification; conversion between scaled oblique echo traces and the equivalent vertical midpoint echo traces; and echo height inversion. The interrelation of these operations, along with the required input data, can be seen in Figure 2.1. This algorithm will generate scaled oblique ionograms that can be used to produce equivalent scaled midpoint vertical ionograms. As shown in this figure, the characteristics of the ionosphere at one or both ends of the path of interest are used to generate an estimate of the midpoint ionosphere. The noise/interference suppression and trace enhancement operations will be performed via a two-stage process utilizing a frequency redundancy technique followed by an adaptive Wiener filter. The Wiener filter will produce a collection of potential trace segments, from the received oblique ionogram. The trace identification algorithm will then determine the most probable set of oblique ionogram traces consistent with both these trace segments and additional information determined from vertical ionograms obtained at the receiving node of the oblique path. In the next stage of development data from an ionospheric model (at present we are considering the International Reference Ionosphere model), will be incorporated with the vertical ionogram data to produce an improved estimate of the midpoint ionosphere.

2.1 Frequency Redundancy Preprocessing

The first noise/interference suppression operation performed on the received oblique ionogram utilizes a frequency redundancy technique. The effectiveness of this technique is based
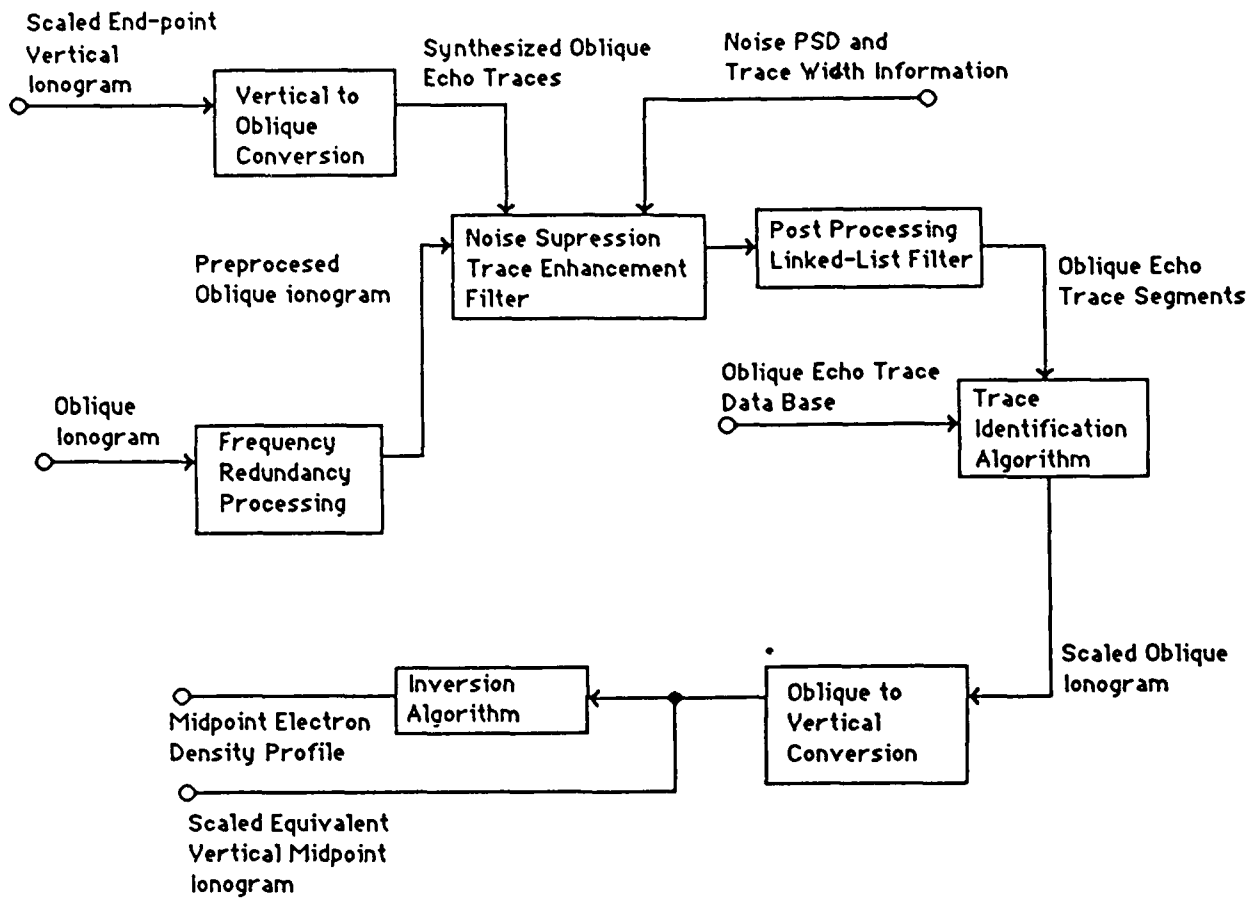
Figure 2.1 Endpoint Vertical Ionogram Based Oblique Ionogram
         Scaling Algorithm

on the fact that the interfering signals produced by spurious radio transmitters are manifested as large amplitude signals at every slant range for a narrow frequency band. Generally an interfering transmitter appears at only one sounding frequency. Since the ionospheric phenomena of interest are essentially constant over several sounding frequencies, an individual sounding frequency (e.g. 25 kHz) step with the highest signal-to-noise ratio within a predetermined frequency interval (e.g. 100 kHz) can be used to represent that entire interval. The result is a relatively noise/ interference-free ionogram with information content equivalent to an ionogram obtained with larger (e.g. 100 kHz) frequency steps. In the preliminary data set 100 kHz oblique ionograms were generated from 50 kHz oblique sounding data by selecting the 50 kHz channel with the highest signal-to-noise ratio from pairs of adjacent 50 kHz soundings. In the proposed operational system a 100 kHz oblique ionogram will be generated from 25 kHz sounding data by selecting the highest signal-to-noise ratio channel from each set of four adjacent 25 kHz soundings.

2.2 Noise/Interference Suppression and Trace Enhancement

The subsequent noise/interference suppression and trace enhancement algorithm uses a minimum-mean-square Wiener filtering technique [Andrews and Hunt, 1969]. This necessitated the development of an appropriate mathematical model for synthesis of the received oblique ionograms from the leading edge components of interest, an oblique-trace spread filter, and any residual noise/ interference present in the preprocessed oblique ionogram. The details of this model are illustrated in Figure 2.2. The preprocessed oblique ionogram, $p_0(t,f)$, is modeled as the sum of a noise/ interference-free "ideal" oblique ionogram, $i_0(t,f)$, and a noise/ interference signal, $n(t,f)$. The "ideal" oblique ionogram, i.e. the oblique trace echo, is modeled as the response of a linear shift-

Oblique Echo Trace
Pulse Width Generation
Filter

$n(t,f)$
Residual
Noise/ Interference
Signal

$h_s(t,f)$

$le_0(t,f)$

Leading Edge of
Oblique Echo Trace

$i_0(t,f)$
Noise/Interference
Free Oblique
Ionogram

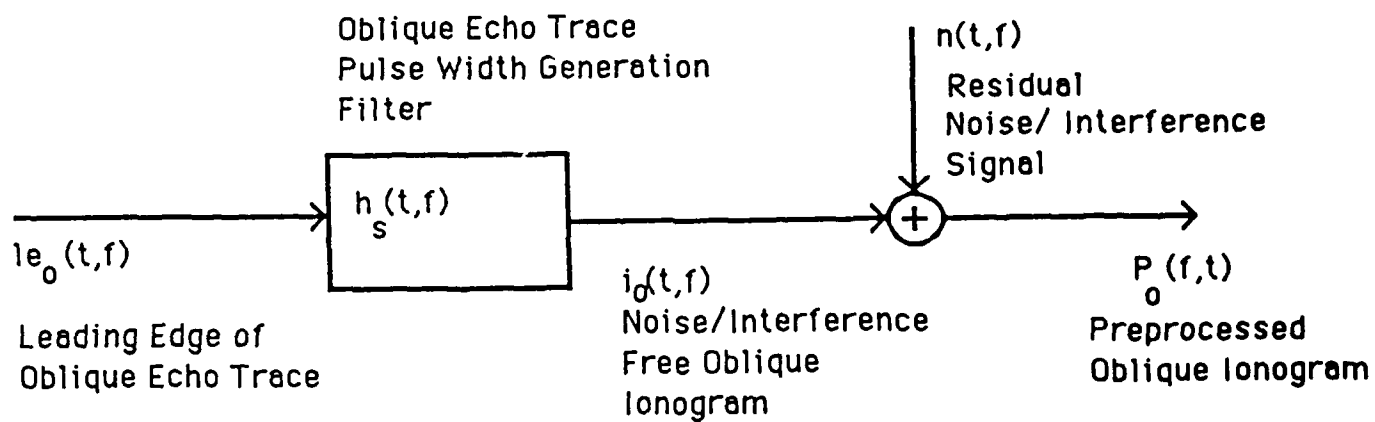$P_0(f,t)$
Preprocessed
Oblique Ionogram

Figure 2.2   Received Oblique Ionogram Synthesis Model

6

invariant oblique-trace spread filter, with impulse response $h_s(t,f)$, to the desired leading edge of the oblique echo trace, $le_o(t,f)$. To implement a minimum-mean-square Wiener filter that can produce an optimal estimate of the leading edge of the oblique ionogram from the preprocessed oblique ionogram, the noise/interference and the leading edge signals are assumed to be stationary random processes of known power spectral density. In addition the oblique-trace spread filter impulse response $h_s(t,f)$ must be known. The function $h_s(t,f)$ generates the pulse width of the transmitted RF pulses and is easily constructed. The average noise function $n(t,f)$, or the corresponding power spectral density $P_n(\omega_t,\omega_f)$, can be obtained by averaging a number of oblique ionograms that do not contain echo traces (i.e. "ionograms" obtained with the DORIS receive subsystem but with the DORIS transmitter off). With these data the two-dimensional frequency domain optimal noise/interference suppression and leading edge enhancement filter is:

$$H(\omega_t,\omega_f) = \frac{H_s{}^*(\omega_t,\omega_f)\, P_{le}(\omega_t,\omega_f)}{\left|H_s(\omega_t,\omega_f)\right|^2 P_{le}(\omega_t,\omega_f) + P_n(\omega_t,\omega_f)}$$

where $P_{le}(\omega_t,\omega_f)$ is the power spectral density of the leading edge of the oblique ionogram which of course is not known, $P_n(\omega_t,\omega_f)$ is the power spectral density of the residual noise/interference signal and $H_s(\omega_t,\omega_f)$ is the two-dimensional Fourier transform of the oblique-trace spread filter impulse response $h_s(t,f)$. It is tempting to use a generic function $P_{le}(\omega_t,\omega_f)$ to represent all oblique ionograms but this would limit the effectiveness of this technique, given that the filter would only produce a minimum-mean-square estimate of the leading edge signal relative to all possible oblique ionograms. To overcome this drawback an adaptive approach is used. The specific differences between oblique ionograms can be attributed to three major factors: diurnal variations; geographical orientation of the specific oblique

path and ionospheric disturbances. Since all three of these factors would be manifested in the vertical ionograms obtained at the ends of the oblique path, the scaled vertical ionogram at the receiving end of the oblique link is used to estimate the leading edge of the oblique ionogram for that specific path at a specific time. An improved estimate of $P_{le}(\omega_t, \omega_f)$ could be obtained by using the vertical ionograms from both terminal points. This would increase the software and communication requirements since the IONHT message from the transmitter site would have to be sent to the receiver site via the Air Weather Service Automated Weather Network.

3.0 EVALUATION OF OBLIQUE TRACE ENHANCEMENT ALGORITHM

The performance of the oblique ionogram trace enhancement algorithm was evaluated using a set of ionograms obtained during days 90-98 (March 30 - April 7) of 1988. The oblique path was approximately 1800 km long with the transmitting Digisonde 256 in Goose Bay, Canada and the corresponding receiving system at Millstone Hill Observatory in Westford, MA. The Goose Bay station used a horizontal log periodic transmit antenna, while the Millstone Hill station used the standard Digisonde seven loop receive antenna array. The protocol used to collect data produced sets of three ionograms, consisting of a vertical ionogram, an oblique ionogram, and a vertical ionogram, 15 minutes apart. Synchronization of the two stations, which is required for. oblique ionograms, was performed manually. The vertical ionograms scanned the frequency range from 1 to 10 MHz with 100 kHz sounding frequency increments, while the oblique ionograms scanned over a frequency range of 4 to 18 MHz, using 50 kHz sounding frequency increments. The results presented in Figures 4 through 14 were generated using an Apollo 660 workstation, with the required algorithms implemented in Fortran.

A representative data set is presented in Figure 3.1. The upper panel shows the amplitudes, as determined by the Digisonde 256 MMM technique, of a vertical-oblique-vertical ionogram set, obtained at the times indicated. The pseudocolor intensity scale used for all amplitude displays is presented at the extreme left of Figure 3.6, ranging from black for the smallest amplitude to white for the largest amplitude. The lower panel of Figure 3.1 shows the corresponding polarizations, with the vertical ordinary polarization displayed in red, the vertical extraordinary polarization displayed in green; the oblique ordinary polarization is displayed in yellow and the oblique extraordinary polarization displayed in blue.
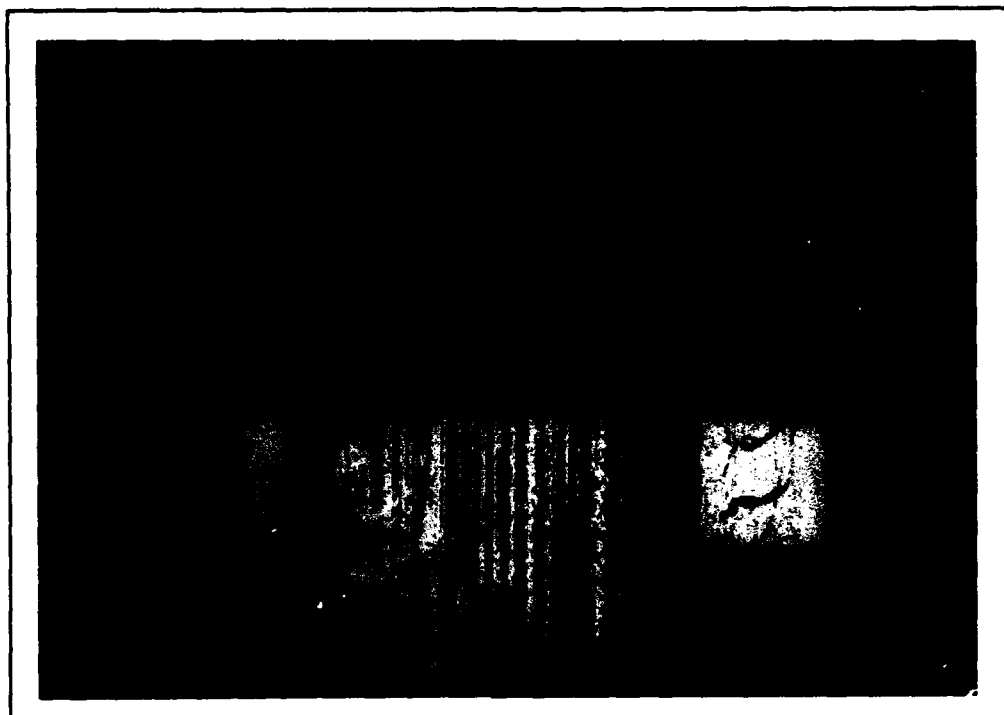
Figure 3.1 Representative test data. Upper series consists of the amplitude, in Digisonde 256MMM format, of a vertical, oblique and vertical ionogram set obtained at the times indicated. The lower series are the corresponding polarizations.

The oblique ionograms also contained local vertical echo traces that were removed before noise/interference suppression or trace enhancement was performed. An estimate of the vertical echoes in the oblique ionogram was obtained by performing a logical NAND operation on all range bins tagged as part of either the ordinary or extraordinary traces of the adjacent vertical ionograms. This estimate was used as a mask to remove the vertical component in the oblique ionogram. Subsequently any removed range bind was replaced with the most probable amplitude for that frequency. The results of this process are shown in Figure 3.2. The third hop vertical component in the oblique ionogram was not present in the corresponding vertical ionograms and hence was not suppressed.

The effects of the frequency redundancy preprocessing can be seen in Figure 3.3. Each set of 50 kHz sounding frequencies was examined and the most interference free frequency was used to produce the 100 kHz ionogram seen on the right of Figure 3.3.

The *implementation of the* Wiener filter required an estimate of the power spectral density of the interfering transmitters. This was obtained by recording 50 interference-only ionograms over a period of five days approximately two hours apart. This data base for estimating $P_n(\omega_t,\omega)$ is appropriate if the total number of interferers is approximately constant with time. The respective power spectral densities were computed and averaged together to produce the data presented in Figure 3.4. The strong components along the ω_f axis indicates that the interfering transmitters produce uniform amplitude signals at all range bins at a particular sounding frequency.

The power spectral density of the leading edge of the oblique echo traces was computed by first synthesizing an oblique leading edge signal from the ARTIST scaled vertical data, via the secant law [Davies, 1969], for the vertical ionogram immediately prior to the oblique ionogram of interest. For a given frequency f_v
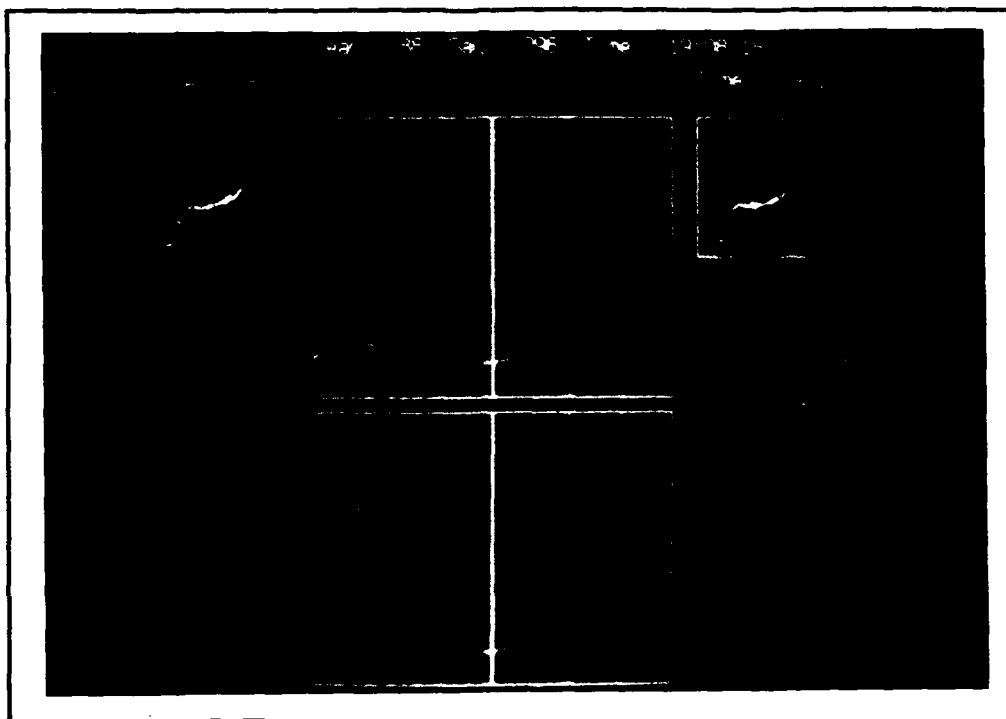
Figure 3.2 Representative ionogram set in upper panel. Lower panel is the corresponding oblique ionogram with the local vertical ionogram suppressed.
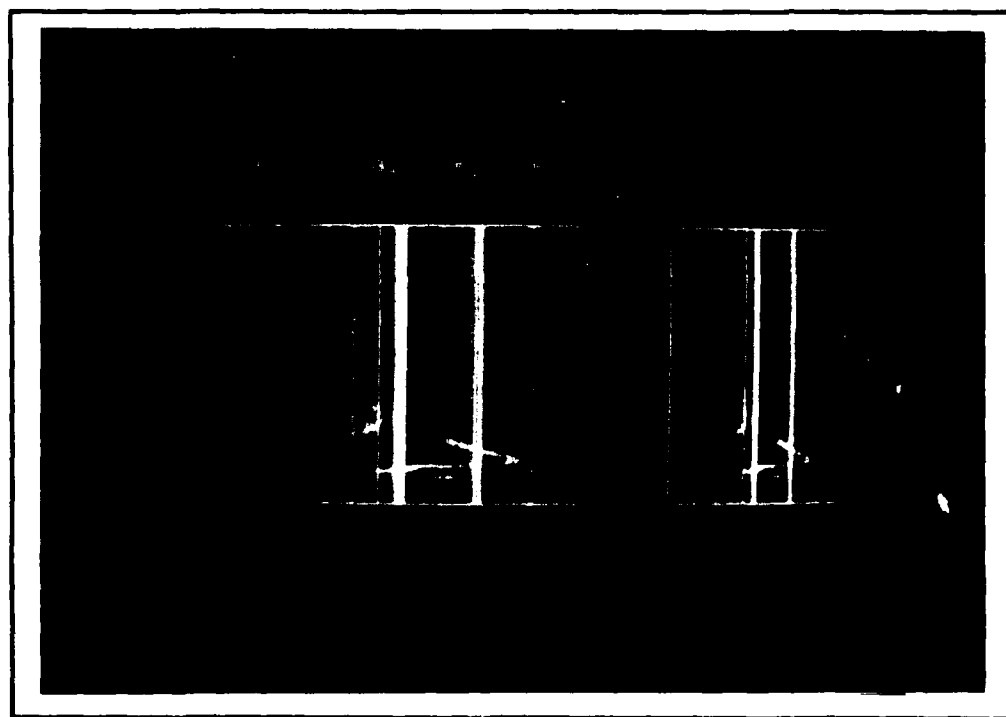

Figure 3.3 Original 50 KHz oblique ionogram and corresponding 100 KHz ionogram produced via frequency redundancy technique.

12

reflected vertically at a virtual height h', the corresponding oblique frequency f_o reflected at the same virtual height is $f_o = f_v \, \Phi_o$, where Φ_o is the obliquity factor given as $\Phi_o = k \sec \phi$, Φ being the zenith take off angle. The factor k varies from 1.0 to 1.1 for distances from 0 to 3000 km [Wilder, 1955]. Considering curved earth geometry the angle Φ is given by

$$\phi = \frac{\sin (\theta / 2)}{1 + \dfrac{h'}{a} - \cos (\theta / 2)}$$

where a is the earth's radius (6370 km), θ is the angle at the center of the earth subtended by the endpoints of the oblique path, and h' is the vertical reflection height. The magnitude squared of the two-dimensional Fourier transform of the synthesized oblique traces was used as the desired power spectral density. Figures 3.5 and 3.6 show these results for the representative data set. In the scaled vertical and oblique data in Figure 3.5, the E trace is presented in yellow and the F trace in white. The data in Figure 3.7 allow comparison of the actual vertical ionogram with the ARTIST scaled data, and the actual oblique ionogram with the synthesized scaled data. The synthesized oblique data, superimposed on the actual oblique data in the right panel, is quite similar in shape but shifted up in frequency slightly. As expected, since the scaled vertical data is derived from the vertical ordinary trace, the synthesized oblique data more closely matches the corresponding oblique ordinary trace.

The Wiener filter behavior is seen in Figure 3.8. The interfering transmitters produce the same strong signal along the ωf axis that was evident in the interference/noise power spectral density. After processing by the filter (shown in the lower two center panels) the oblique traces (upper right panel) are enhanced (i.e. the interference has been suppressed and the leading edge of the oblique ionogram is more apparent). In the expanded view of the
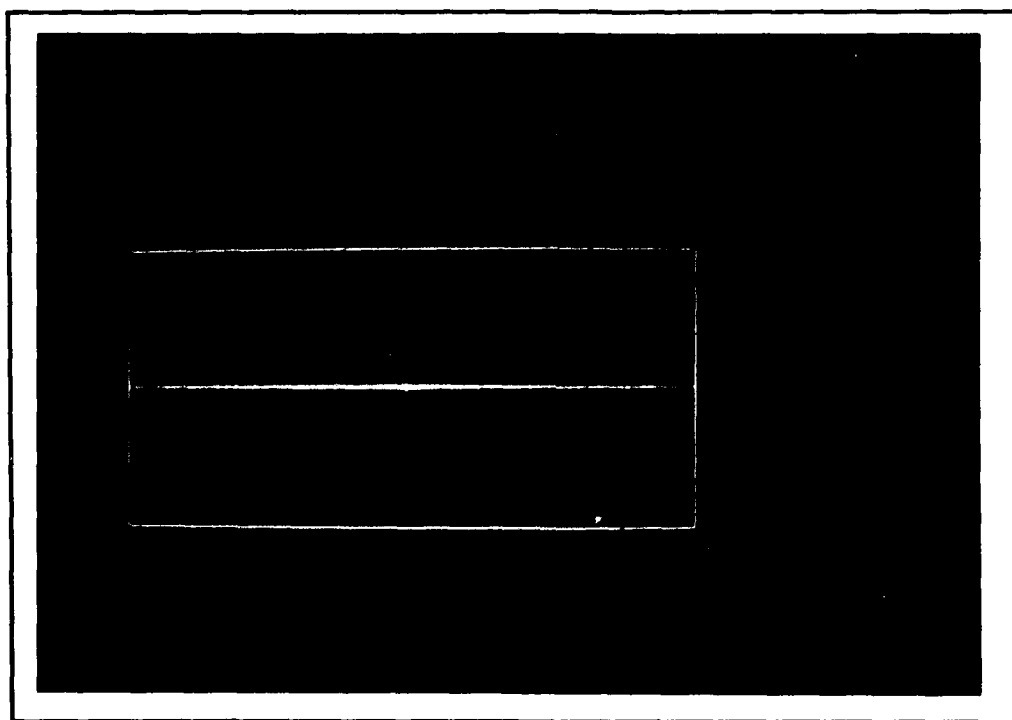
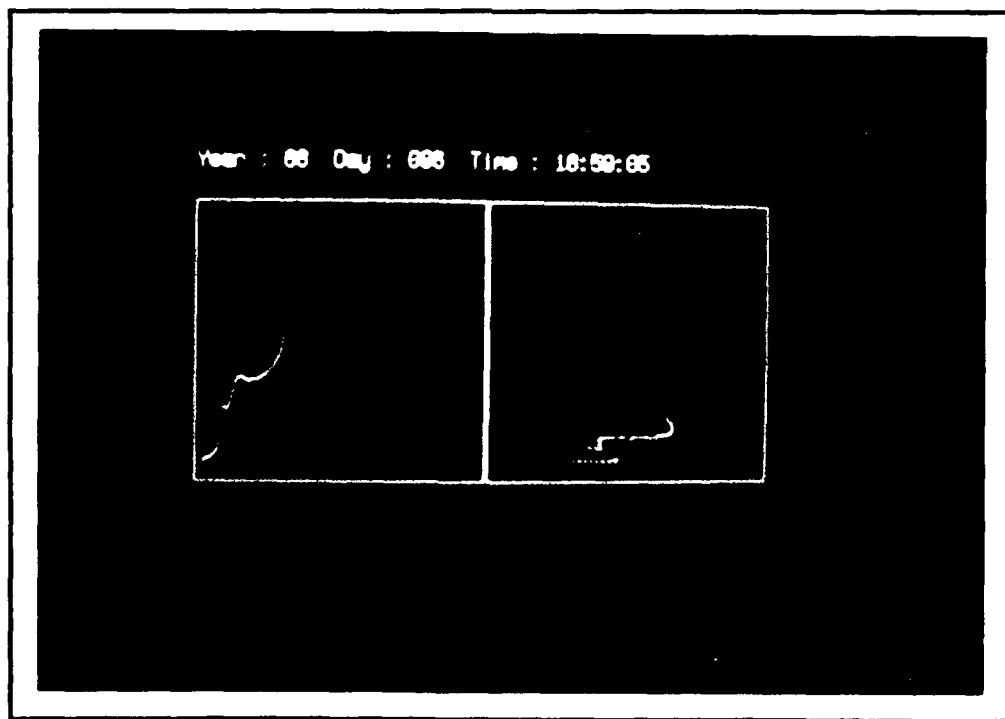**Figure 3.4** Power spectral density of interfering transmitters and additional noise.

Figure 3.5 ARTIST scaled vertical ionogram and corresponding scaled oblique ionogram synthesized via secant law.
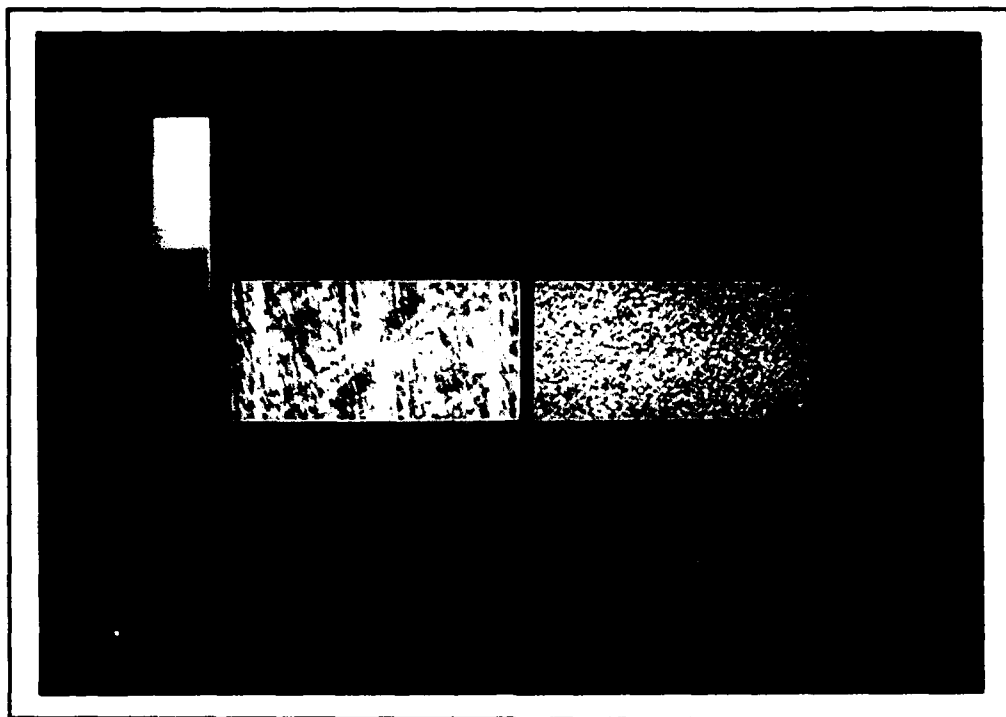
14

Figure 3.6 Synthesized scaled oblique ionogram, magnitude, phase and magnitude squared (power spectral density) of corresponding two-dimensional Fourier transform (clockwise from upper left panel).
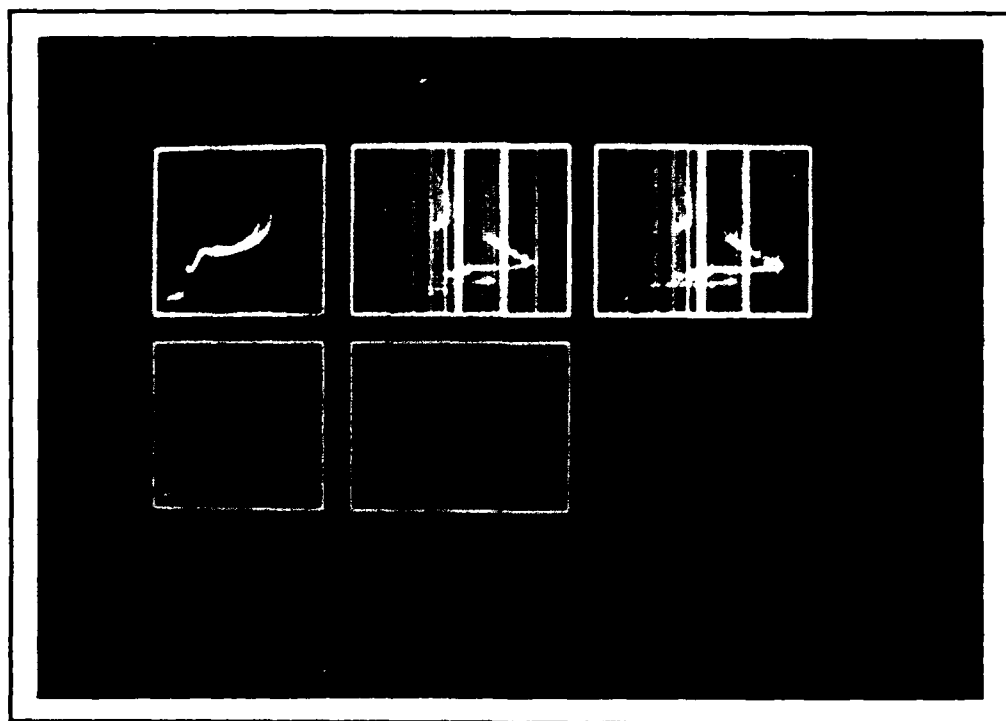

Figure 3.7 Vertical ionogram and corresponding **ARTIST** scaled ionogram (upper and lower left panel respectively), preprocessed oblique ionogram and corresponding scaled oblique ionogram synthesized via secant law (upper and lower center panel respectively), synthesized scaled oblique ionogram superimposed on actual oblique ionogram (upper right panel).

15

Figure 3.8 Preprocessed oblique ionogram and corresponding two dimension Fourier transform magnitude and phase (from top, left panel), Wiener filtered version o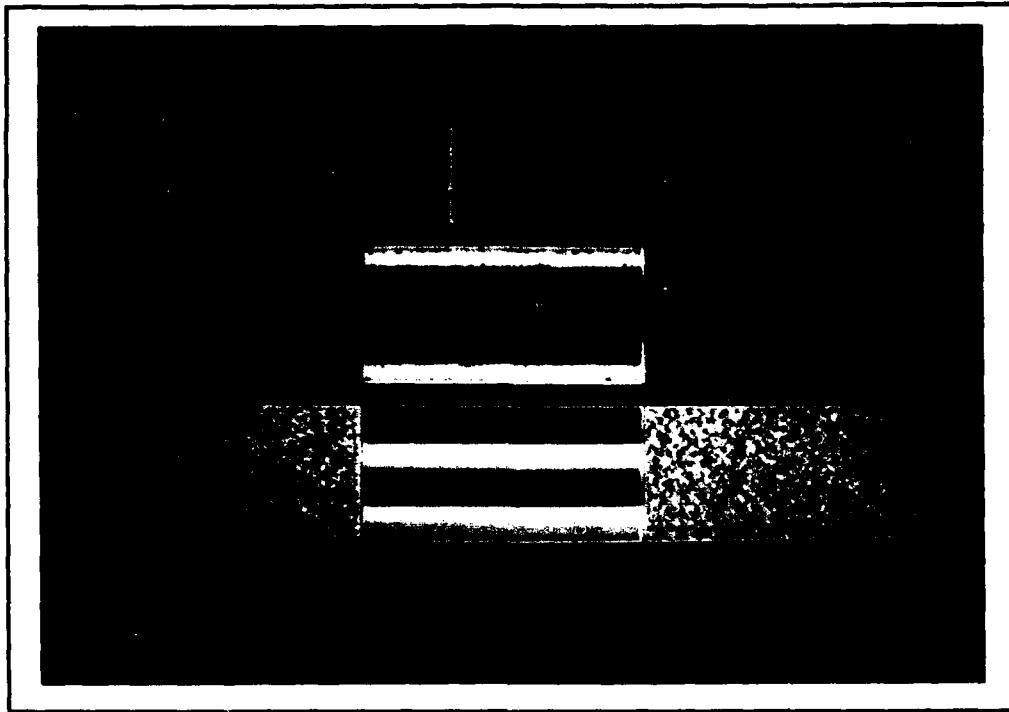f preprocessed oblique ionogram and corresponding two dimension Fourier transform magnitude and phase (from top, right panel), Wiener filtered version superimposed on preprocessed oblique ionogram, magnitude and phase of Wiener filter (from top, center panel).
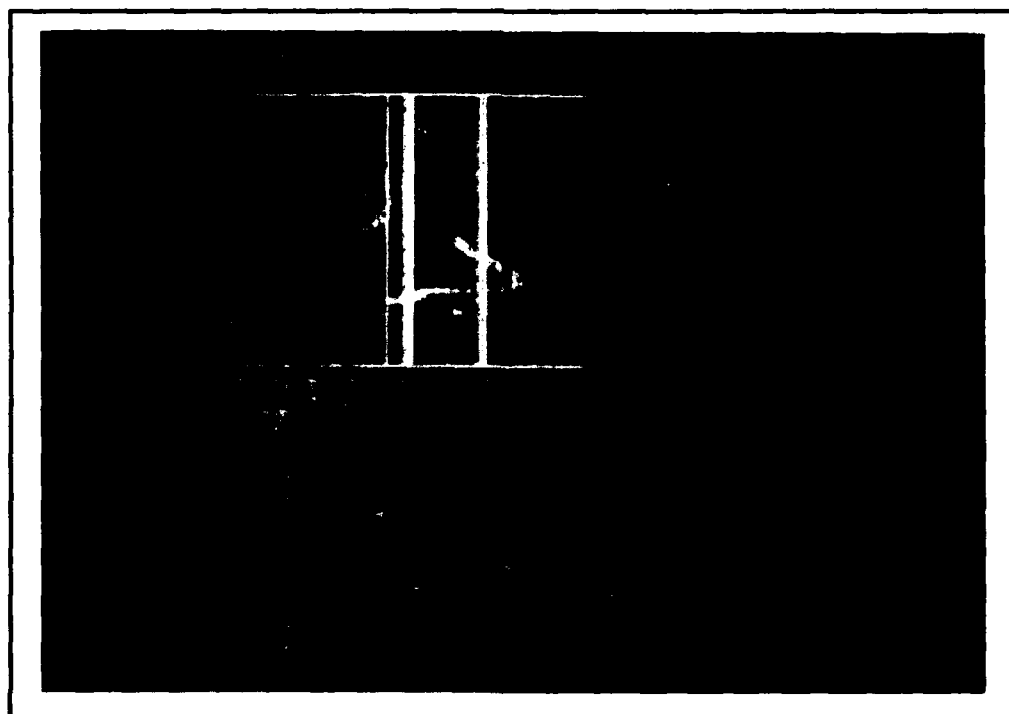

Figure 3.9 Preprocessed oblique ionogram and corresponding Wiener filtered version (upper and lower panels respectively).

original oblique data and the resulting enhanced trace segments, presented in Figure 3.9, an undesirable artifact is present in the enhanced trace data, primarily at those sounding frequencies where the original oblique data was corrupted by the local vertical echoes. In addition to the residual signals resulting from the incomplete suppression of the local vertical echoes, these sounding frequencies also contain multiple hop oblique signals. Since neither of these components are accounted for in the Wiener filter the resulting "impulse-like" noise is produced. To a lesser extent other low signal-to-noise regions of the oblique ionogram also exhibit this processing artifact. A nonlinear post-processing linked-list filter [Fu, 1974] was developed to reduce this artifact. The filter rejected as noise any group of contiguous pixels; i.e. pixels adjacent in either frequency or virtual height, of less than a predetermined threshold. In the data presented in Figures 3.10 and 3.11, contiguous groups of three or more pixels were considered as potential oblique trace segments.
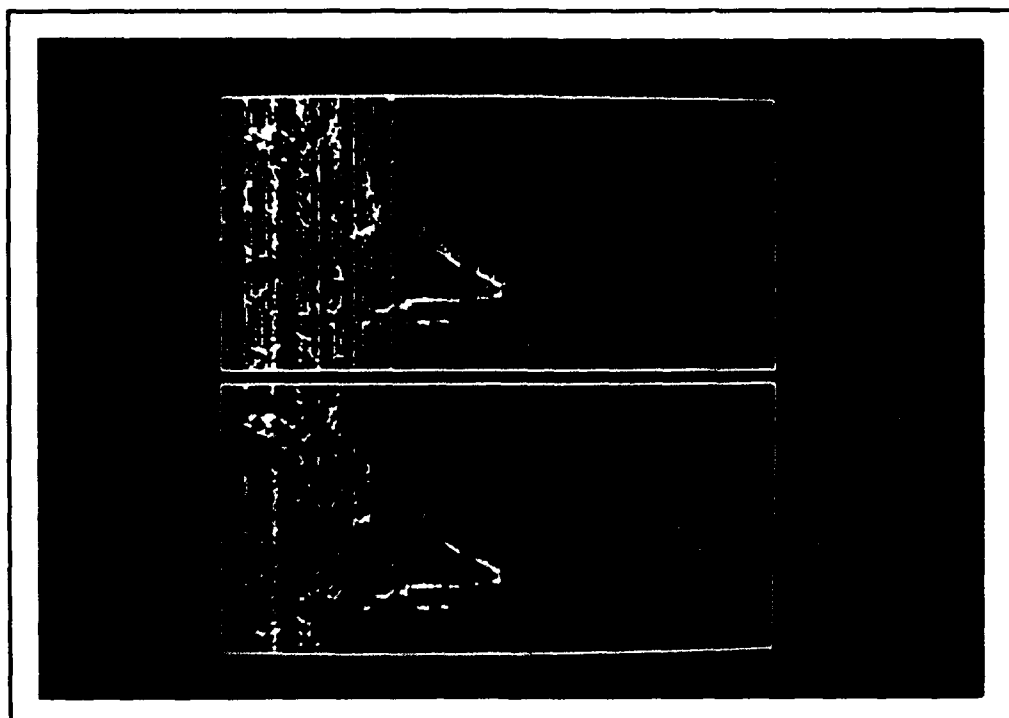
Figure 3.10 Wiener filtered oblique ionogram and corresponding linked-list post-processed version (upper and lower panels respectively).
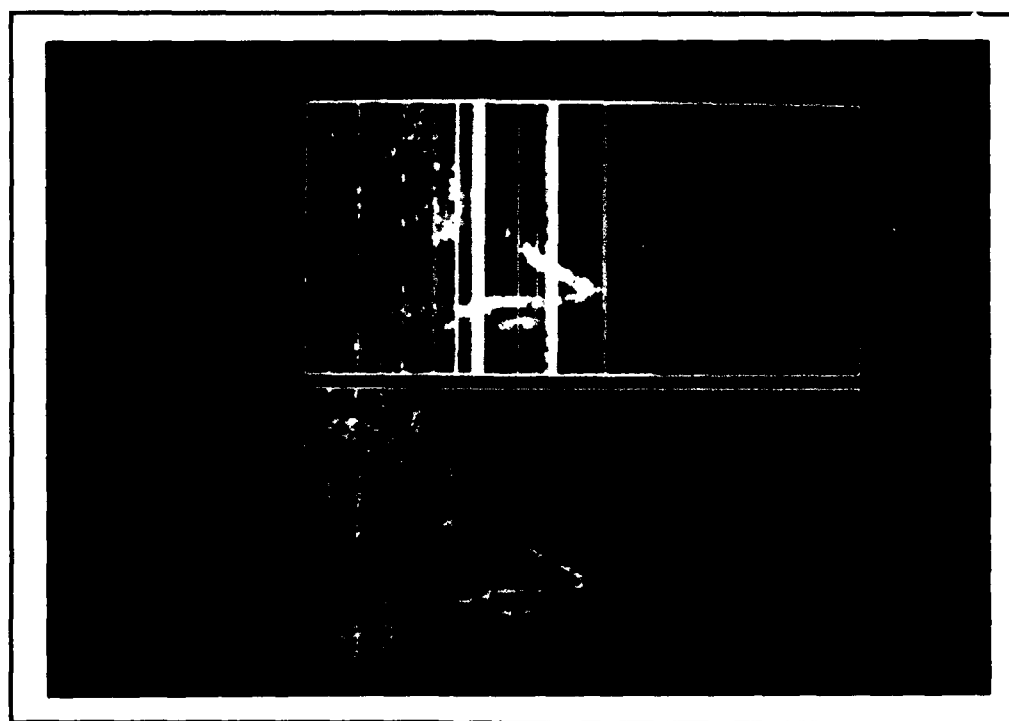

Figure 3.11 Linked-list post-processed oblique ionogram superimposed on actual oblique ionogram and linked-list post-processed oblique ionogram (upper and lower panels respectively).

4.0 FUTURE DEVELOPMENT

At present, the noise/interference and trace enhancement components of the endpoint vertical ionogram based oblique scaling algorithm have been implemented and tested using a limited set of oblique ionograms. A more extensive set of oblique ionograms will be collected both to further test these algorithms and to develop the trace identification algorithm. The trace identification algorithm will use syntactic, also referred to as structural, pattern recognition techniques [Fu, 1974] to determine the most probable set of oblique ionogram traces consistent with both these trace segments and additional information determined from vertical ionograms obtained at one or both ends of the oblique path. One of the potential weaknesses of the endpoint vertical ionogram based oblique scaling algorithm, as proposed in Figure 2.1, is that for long paths, in particular those that cross the terminator, there will be significant differences between the endpoint and midpoint ionosphere. This can be addressed by using adaptive techniques, as shown in Figure 4.1. In this approach, a model-predicted endpoint ionosphere is compared with the measured endpoint ionosphere. Based on this comparison, the model parameters are adjusted to produce results consistent with the measured data. This endpoint model correction is then used to correct the model ionosphere at the midpoint. The synthesized oblique traces produced in this manner can then be used in place of the synthesized oblique traces generated by converting scaled endpoint echo traces via the modified secant law.
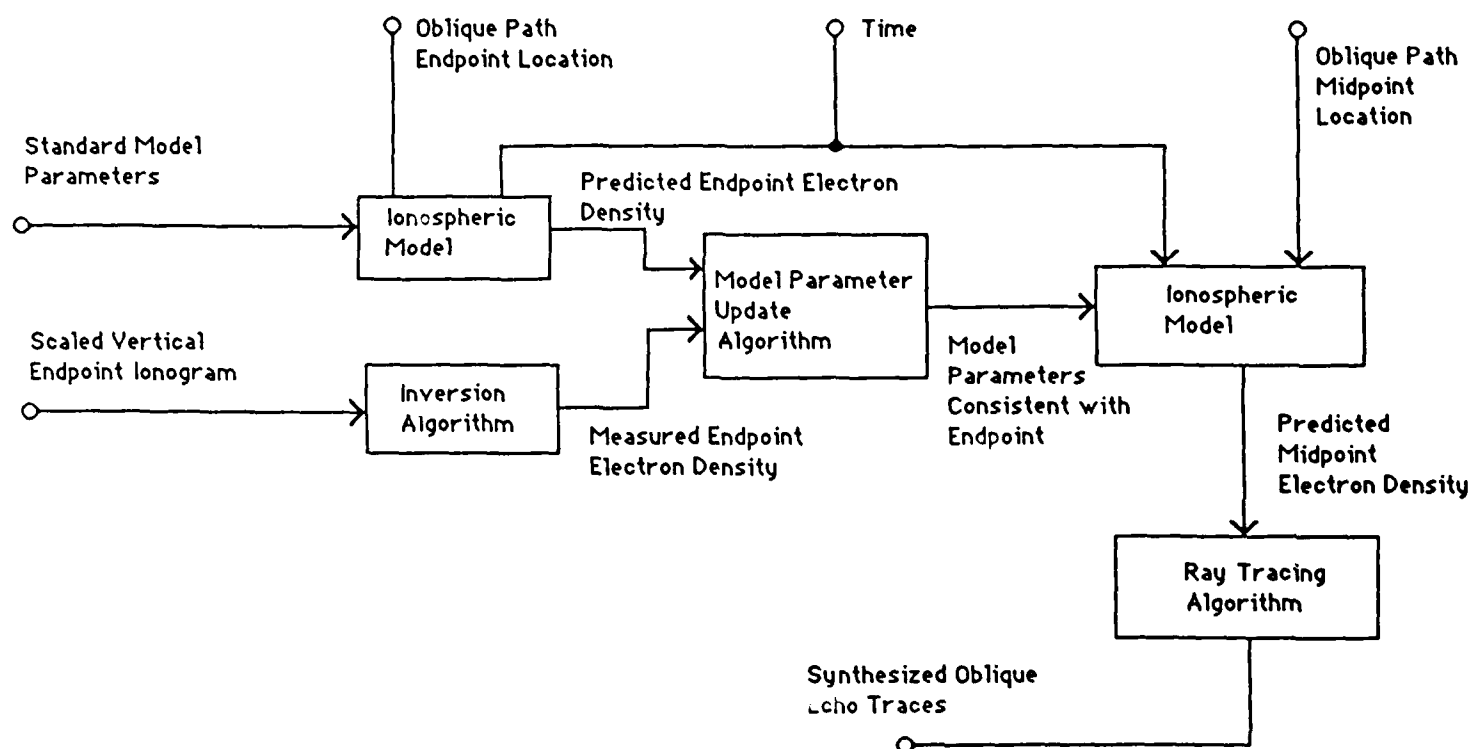
Figure 4.1   Adaptive Model-Based Oblique Echo Trace Algorithm

5.0 DORIS MILESTONES

The milestone charts for the development of the oblique ionogram scaling algorithm and the overall DORIS project are found in Figures 5.1 and 5.2 respectively. At present, the frequency redundancy preprocessing algorithm, noise suppression and trace enhancement algorithm and post processing linked list algorithm have been implemented and tested as described in Section 4.0. A more extensive oblique ionogram data set is being collected, and after the initial oblique echo trace identification algorithm is developed, this data set will be used to study the performance of the endpoint vertical ionogram based oblique scaling algorithm. This algorithm will produce equivalent digital midpoint vertical ionograms of virtual height vs. sounding frequency with 2.5 km height resolution and 100 kHz frequency resolution. These results will be compared with actual vertical ionograms at the midpoint of the oblique path, that will also be recorded during the collection of the oblique ionogram data set. The oblique path used for these experiments will have the transmitting Digisonde 256 at Goose Bay, Labrador, the receiving system at Wallops Island, Virginia (or vice versa), and data from the East Coast OTH-B Radar quasi-vertical ionosonde (Moscow to Columbia Falls, Maine) to determine the corresponding midpoint vertical ionograms.
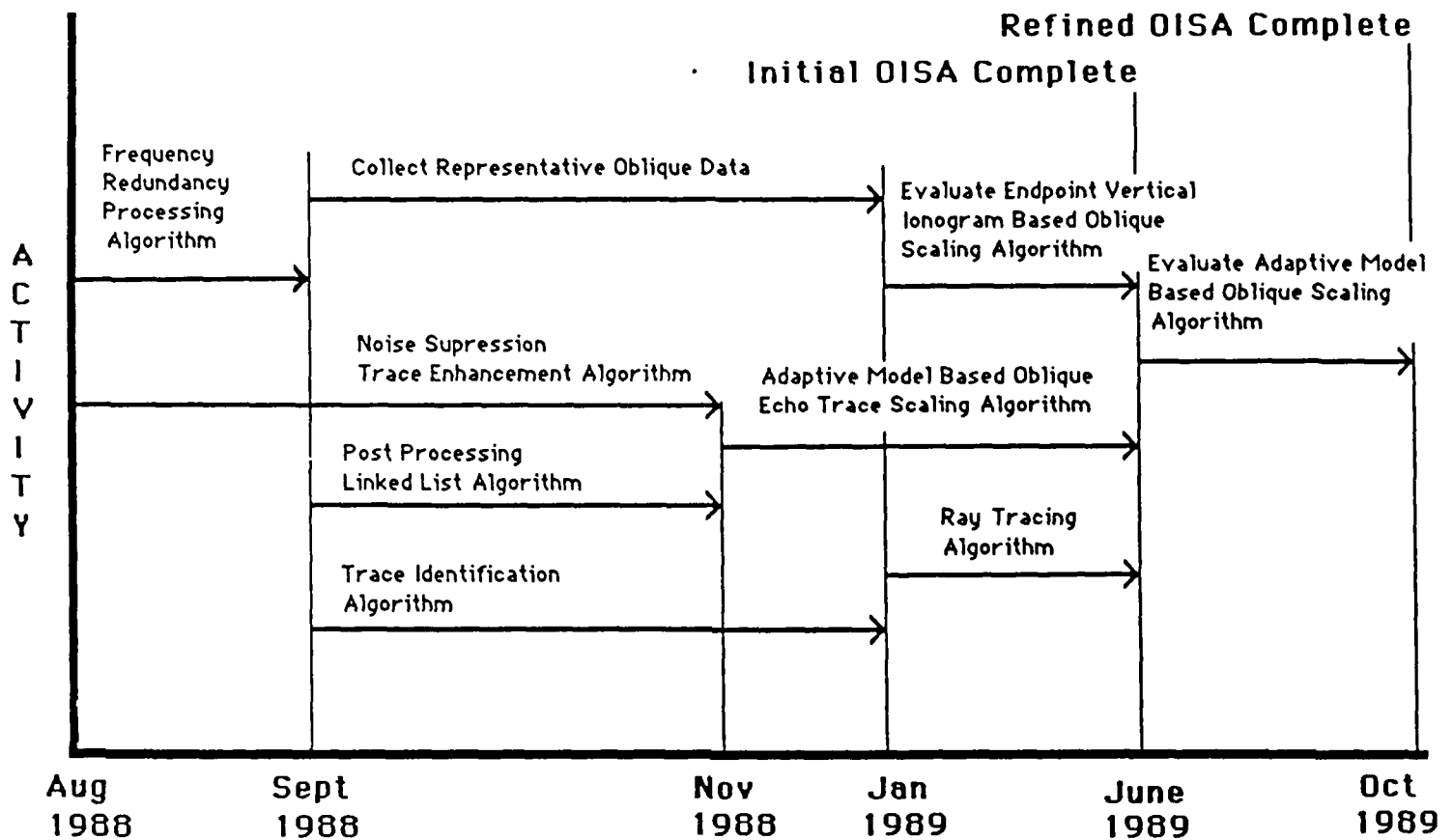
Figure 5.1   Milestone Chart for Oblique Ionogram Scaling Algorithm

22

Digital Oblique Remote Ionospheric Sounding

FY88				FY89				FY90				FY91
4th Qtr	1st Qtr	2nd Qtr	3rd Qtr	4th Qtr	1st Qtr	2nd Qtr	3rd Qtr	4th Qtr	1st Qtr	2nd Qtr	3rd Qtr	4th Qtr	1st Qtr

October 20, 1988

Preliminary Oblique Sounding

Transmit Antenna Installed at Wallops Island
Timing Standards Installed at Wallops Island and Goose Bay

Two Week Initial Experiment

Automatic Synchronization Card Complete

Automatic Synchronization Firmware Complete

Automated System Ready for Test

Two Week Field Experiment

USAF Program Review

Go/No-Go Decision

Compare Receive Antennas

Test Goose Bay to Wallops Island One Direction Only

Upgrade Bermuda Hardware

Two Week Test Wallops Island to Bermuda

One Week DORIS Demonstration

Initial OISA Complete (Offline)

Refined OISA Complete (Offline)

Test Real Time OISA

Development of OISA
(Oblique Ionogram Scaling Algorithms)

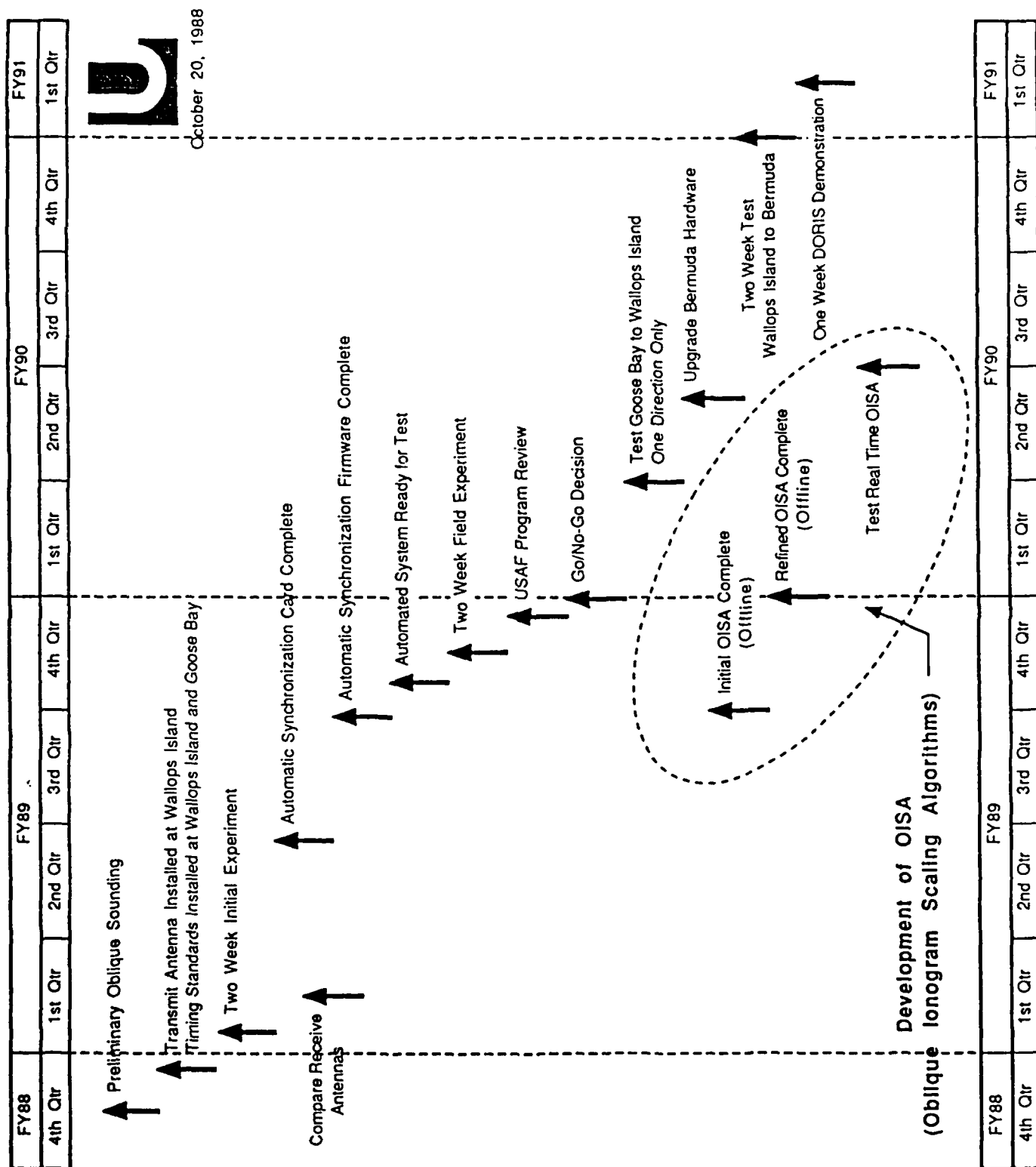| FY88	FY89				FY90				FY91
4th Qtr	1st Qtr	2nd Qtr	3rd Qtr	4th Qtr	1st Qtr	2nd Qtr	3rd Qtr	4th Qtr	1st Qtr

Figure 5.2

23

6.0 REFERENCES

1. Andrews, H. C. and B. R. Hunt, "Digital Image Processing," Prentice-Hall Publishing Co., 1969.

2. Davies, K., "Ionospheric Radio Waves," Blaisdell Publishing Co., 1969.

3. Fu, K. S., "Syntactic Methods in Pattern Recognition," Academic Press, 1974.

4. Wilder, B., "Some Results of a Sweep-Frequency Propagation Experiment Over a 1100 km East-West Path," J. Geophys. Res. 60, 395, 1955.